Can we predict the microstructure of a non-woven flax/PLA composite through assessment of anisotropy in tensile properties?

Delphin Pantaloni, Lea Ollier, Darshil U. Shah, Christophe Baley, Eric Rondet, Alain Bourmaud

▶ **To cite this version:**

Delphin Pantaloni, Lea Ollier, Darshil U. Shah, Christophe Baley, Eric Rondet, et al.. Can we predict the microstructure of a non-woven flax/PLA composite through assessment of anisotropy in tensile properties?. Composites Science and Technology, 2022, 218, 10.1016/j.compscitech.2021.109173 . hal-04585217

HAL Id: hal-04585217
https://hal.science/hal-04585217v1

Submitted on 22 Jul 2024

HAL is a multi-disciplinary open access archive for the deposit and dissemination of scientific research documents, whether they are published or not. The documents may come from teaching and research institutions in France or abroad, or from public or private research centers.

L'archive ouverte pluridisciplinaire **HAL**, est destinée au dépôt et à la diffusion de documents scientifiques de niveau recherche, publiés ou non, émanant des établissements d'enseignement et de recherche français ou étrangers, des laboratoires publics ou privés.

Distributed under a Creative Commons Attribution - NonCommercial 4.0 International License

Version of Record: https://www.sciencedirect.com/science/article/pii/S0266353821005297
Manuscript_243736827b96f7e451927793b6ef592a

Can we predict the microstructure of a non-woven flax/PLA composite through assessment of anisotropy in tensile properties?

Delphin Pantaloni[1], Léa Ollier[2], Darshil Shah[3], Christophe Baley[1], Eric Rondet[2] and Alain Bourmaud[1]

1: Université de Bretagne-Sud, IRDL, CNRS UMR 6027, BP 92116, 56321 Lorient Cedex, France

2 : UMR QualiSud, Université de Montpellier, CIRAD, l'Institut Agro - Montpellier SupAgro, Université d'Avignon, Université de La Réunion, Montpellier, France

3: Centre for Natural Material Innovation, Department of Architecture, University of Cambridge, Cambridge CB2 1PX, United Kingdom

* Corresponding author: delphin.pantaloni@univ-ubs.fr Tel.: +33-2-97-87-45-18

Abstract

Flax/Poly-(lactide) non-woven composites are an alternative to conventional glass/poly-(propylene), offering a potentially lower environmental impact solution for the automotive industry. To understand this complex material, its detailed architecture and void distribution are examined through 3D microtomography. Anisotropy in fibre orientation is also observed, further verified through off-axis tensile tests. Then micro-mechanics and laminate theory are used, taking into account fibre orientation distribution, to predict mechanical properties and compare with experimental measurements. Even though some deviation is observed at off-axis angles greater than 45°, we report that off-axis tensile tests (property) can be used to predict fibre orientation (structure) in industrial production facilities as a simple means of quality control and tailored design of new non-woven preforms.

Keywords

© 2021 published by Elsevier. This manuscript is made available under the CC BY NC user license
https://creativecommons.org/licenses/by-nc/4.0/

A. Natural fibre composites ; B. Mechanical properties ; C. Anisotropy ; D. X-ray tomography ; B. Porosity/void

1. Introduction

Due to their lower environmental impact [1] and competitive specific mechanical properties [2], flax fibres have replaced glass fibres in some automotive parts, such as interior panels [3]. Manufactured from non-woven preforms, these parts are thermo-compressed to a near-net shape. Several processes are available to manufacture non-woven preforms, among which spunlacing and needle-punching are common [4]. In addition, thermoplastic polyolefins, such as poly-(propylene) (PP), are currently used as a matrix, leading to the recyclability of any scraps. However, with the emergence of biodegradable thermoplastics, the automotive industry has started to look at alternatives, such as poly-(lactide), which offer industrial composting as an alternative end-of-life scenario [5].

Furthermore, PLA appears to have the advantage to be stiffer than PP with a tangent modulus of 3.8 GPa against 1.4 GPa [6] and to have a quasi-linear tensile behaviour. As matrix properties influence the mechanical properties of the composite, non-woven flax/PLA composites are observed to have higher stiffness at all volume fractions than non-woven flax/PP composites (Figure 1).

While matrix properties are relevant, it is mainly the fibres responsible for composite mechanical behaviour, with their content directly affecting composite stiffness. The non-woven preform manufacturing process will induce fibre orientation anisotropy resulting in different properties in the machine- and cross- directions of a needle-punching line [4]. Neckar and Das [7] studied the orientation of the fibres in non-

48 woven preforms and derived analytical laws related to the manufacturing process
49 used. The fibre orientation in the non-woven preforms could be obtained simply by
50 transparency observation or optical microscopy [8]. Such methods are relevant for
51 mono-constituent non-woven preforms. For composites manufacturing, the non-
52 woven preforms may comprise two types of fibres, the reinforcement and the matrix.
53 Other methods have to be used as only the reinforcement fibre orientation needs
54 measurement (as the matrix fibres will melt) to investigate the effect of fibre
55 architecture on composite mechanical properties. Graupner et al. [9] used a
56 synchrotron radiation-based micro-computer tomography approach to obtain cellulose
57 fibre orientation in PLA composites. Another non-destructive method is to use
58 ultrasound scanning, leading to the measurement of fibre orientation and ply spacing,
59 fibre volume fraction and porosity distribution [10]. In both cases, computation is
60 required to extract fibre orientation from the raw data, leading orientation
61 information on the composite volume and not only on the surface.
62 The orientation of the flax in the composite (or the non-woven preform) is of great
63 industrial interest. It can be used as a quality controller for industrial production or for
64 pilot tests to validate machinery set-up to obtain specific fibre orientations and
65 tailored architectures. The latter is of interest as highly aligned non-wovens offer a
66 viable route, technically and economically speaking, to obtain anisotropic preforms
67 with mechanical properties intermediate to quasi-isotropic non-wovens and
68 unidirectional mats.
69 Once orientation frequency distribution is known, several theories exist to predict non-
70 woven mechanical properties. The first approach is to modify the rule-of-mixtures (1)

by including a corrective factor η_o (2) [11], where *E* and *V* denote stiffness and volume fraction respectively, and subscripts NW, *f* and *m* denote non-woven composite, fibre constituent and matrix constituent, respectively. The parameter p_n is the appearance frequency of the angle represented by θ_n.

$$E_{NW} = \eta_o . E_f . V_f + E_m . V_m \quad (1)$$

$$\eta_o = \sum_n p_n . cos^4(\theta_n) \quad (2)$$

In the above approach, even though the fibre orientation is taken into account, the shear contribution is not taken into account, nor are the anisotropic properties of the reinforcement. Halpin and Pagano [12] developed a more precise method by assimilating randomly oriented fibrous composites to a laminate. By considering symmetric laminate with a thickness weighted with the fibre orientation frequency, they showed a good mechanical prediction.

A third constituent important to tackle is the porosity value. The compaction of the non-woven could be controlled, leading to low or higher porosity content, to tailor mechanical or acoustic properties [13]. Focussing on fully-compressed composites, porosity is still present due to manufacturing and should not be neglected as it influences mechanical properties. Their distribution and shape are also reported to be important [14]. Looking specifically at natural fibres, Madsen et al. discussed the porosity distribution inside hemp thermoplastic composites [15] and its influence on composite stiffness [16]. Thus, fibre orientation, fibre anisotropy and porosity appear to be key structural parameters required in precisely describing a non-woven composite, all of them impacting non-woven composite mechanical properties.

In this paper, the microstructure (porosity/reinforcement content) and the architecture (fibre orientation) of a flax/PLA non-woven are characterised thanks to X-ray computed microtomographic (X-ray micro-CT) analysis. Off-axis tensile tests are used to characterise the observed anisotropy. Micro-mechanics and laminate theory are used to approximate experimental data. Matching calculated and measured values allows proposing the off-axis mechanical properties as an efficient and simple validation tool to address the fibre orientation in a non-woven composite.

2. Materials and Methods

2.1. Reinforcements

Flax/PLA non-woven preform was provided by Ecotechnilin (Yvetot, France). It was made from 50%/50% weight of scutched flax tows and INGEO™ PLA fibres. Due to the utilisation of flax tow, shives were still present in the non-woven preform. Our non-woven presents a larger proportion of preferential fibres orientations than needle-punched non-wovens due to their manufacturing process: carding and calendaring. The preferential fibres direction is observed on the machine direction (direction of the non-woven preform production). Cross direction refers to the direction perpendicular to the machine direction. Non-wovens with 10% and 30% fibre weight content were also manufactured for comparison. Following, if nothing is indicated, non-woven composite refers to the 50%/50% flax/PLA non-woven.

Unidirectional (UD) and bi-axial (BX) composites were made of 50 g/m² Flax-tape® (Ecotechnilin) and PLA films. This film was made in our laboratory with a process developed in a previous study [6].

2.2. Composite manufacturing

Non-woven composites were made of several preform plies, UD and BX lay-ups were prepared via the film stacking method. Pure PLA plates of both references were also prepared to obtain matrix properties. These lay-ups were dried in an oven at 40°C for 24h under vacuum as flax and PLA are moisture-containing. They were then hot compressed at 200°C with a hydraulic press LabTech Scientific 50T (Labtech, Samutprakarn, Thailand), yielding laminate plates of 20 cm x 20 cm x 2mm. The optimised pressure cycle used is presented in a previous study [6]. A milling machine was used to cut samples for tensile property characterisation.

2.3. Tensile tests

An Instron universal testing machine was used to achieve static tensile tests based on ISO 527-4. A displacement rate of 1mm/min was applied, and the elongation was recorded with a unidirectional extensometer, gauge length taken equal to 25mm. For the pure PLA samples as well as for the UD, a bi-axial extensometer was preferred. For each formulation, at least five samples were tested to obtain mean values and standard deviation. The ultimate strength and strain are recorded as well as tangent modulus. The latter was calculated over a strain of 0.02% to 0.1% as recommended for flax composites [17]. The Poisson's ratio is obtained using the NF EN 2561 standard when the bi-axial extensometer is used.

The same set-up is used, using a bi-axial extensometer and speed of 2mm/min, to do some in-plane shear testing on BX according to ISO 14129. As reported previously [18], the shear modulus is measured between a shear strain of 0.1% and 0.5%.

Pure PLA, UD and BX characterisation is only performed for back-calculation to obtain flax fibres properties.

2.4. Density

The density of our non-woven composite was obtained through a hydrostatic scale using ethanol as the immersion liquid. This method was chosen as suggested by Kergariou et al. [19] for flax/PLA composite. It was used to obtain the density of the composites. Knowing the apparent density of the composite (ρ_c), the volume fraction of porosity (V_p) of each formulation is obtained using equation (3), where W_f is the weight fraction of fibres and ρ_{PLA}, ρ_{flax}, are the density of PLA and flax taken respectively as 1.24 [6] and 1.5 [20]. Porosity results are given as mean values of five samples.

$$V_p = 1 - \left(\frac{1 - W_f}{\rho_{PLA}} + \frac{W_f}{\rho_{flax}}\right).\rho_c \quad (3)$$

2.1. X-ray microtomography (X-ray micro-CT)

The microstructure of the non-woven composites was investigated with a Brucker© SkyScan 1272 high-resolution scanner. The samples were scanned at a nominal resolution of 4,5 µm. The current (50 eV), the intensity (200 µA) of the X-ray beam, and the nature and thickness of filters were selected to obtain a constant signal transmission of 30%. The X-Ray power source (P=U.I) is kept constant at 10W. A camera pixel binning of 4032×2688 was applied. The scanned orbit was 180 degrees with a rotation step of 0.2° adapted to the magnification. Bruker's NRecon® software was used to reconstruct the scan projections into 2D images using the Feldkamp algorithm. Gaussian smoothing, ring artefact reduction and beam hardening correction

were applied. Volume rendered 3D images were generated using an RGBA transfer function in SkyScan CTVox® software. Image analysis was performed using SkyScan CTAn® software. A specific task list analysis was developed to characterise the porosity and the pore size distribution within composites. In that way, two image segmentations were successively carried out on the original image: the first one to define the sample volume of interest (VOI) and the second one, using an automated Otsu algorithm, to define the object volume within this VOI. After image binarisation, structure separation (=pore size) is preceded by skeletonisation in which the two medial pore axes are identified. Then the "sphere-fitting" local thickness measurement is made for all the voxels lying along this axis. In order to determine fibre orientation, a sequence of 12 in-plane cuts on face direction on the 3D render is used to generate 2D images. This method is based on granulometry analysis and was the subject of a previous study [21]. Due to the low contrast – a result of the comparable material densities– between flax and PLA, the 2D images had to be pre-treated with Fiji to obtain binary images before orientation analysis. The pre-treatment process is illustrated in S.I. Figure 1 and validated by comparing the analysis of the orientation of the fibre, with and without pre-treatment, of an optical micrograph, S.I Figure 2.

2.2. SEM

Complementary microstructure observations were performed using a JEOL SEM (JSM-IT500HRSEM) at an acceleration voltage of 3 kV. Before the observation step, gold sputter coating was applied to the samples using an Edward sputter coater (Scancoat6).

3. Results and discussion

3.1. Fine-scale composite volumetric analysis

The behaviour of a composite is predominantly influenced by the matrix, the reinforcement properties and their content. In the case of flax reinforcements, things are more complex as the matrix is not reinforced by one single type of constituent but by at least two: elementary fibres and fibre bundles. Figure 2 presents SEM observations of our non-woven composite. The presence of elementary flax fibres and bundles is confirmed, as well as any preferential orientation. Indeed, non-woven composites are anisotropic as they present higher properties in one direction than another, depending on the preferential orientation of the fibres [4]. However, the microstructure of this non-woven composite is more complex as it also includes porosity and shives. In addition, quantification of fibre orientation is required to describe the non-woven composite architecture, the aim being to understand better and estimate the composite properties.

3.1.1. Porosity analysis

Porosity content of 5.6 ± 3.2 % was measured for the non-woven composite thanks to a hydrostatic balance using ethanol as the immersion liquid. To investigate pore localisation and size, a fine-scale analysis was done by micro-CT. A porosity of 4.5 % was obtained, which is comparable to the immersion method value. It could be observed in Figure 3.c) thanks to the microtomographic 3D view of porosity. Via a quantitative analysis presented in Figure 3.b) a few meso-porosity are highlighted inside the matrix.

On the other hand, there is an important amount of micro-porosity. The latter appears to be mainly located inside bundles and/or in shives. Indeed, shives come mainly from

the xylem tissue, where its main function is to conduct sap [22]. Thus, inside the stem, these cells exhibit a large lumen of several micrometres, potentially visible through micro-CT investigations.

3.1.2. Shives quantification

Regarding the porosity analysis, it appears that shives are a predominant host of micro-porosity. It is observed in Figure 2 and confirmed in Figure 4 that shives inside the non-woven composite had collapsed cells, probably due to the compaction pressure applied during the manufacturing process. Indeed, shives contain less cellulose than elementary flax fibres, 45% of dry matter against 80% respectively [23]. As cellulose is responsible for plant fibres' mechanical properties, it is necessary to quantify this third reinforcement type as it should have mechanical behaviour lower than that of the bundles and elementary fibres. Following manual extraction, 5wt% of shives were extracted for the total non-woven reinforcement weight. Considering a density of 1,430 $kg.m^{-3}$ [24], the volume fraction of shives inside the composite is assessed to be 2.2%, against 43.1% for flax fibres (elementary fibres and fibre bundles). In the following analysis, shives are taken into account by assimilating them into the total flax fibre content at 45.3% by volume.

3.1.3. In-plane orientation of fibres

Finally, a fine-scale description of the non-woven composite architecture should include fibre orientation. Thanks to micro-CT, the orientation was obtained from 12 images, and the mean orientation was calculated. The analysis methods for one image is detailed in Figure 5 b), c), and d). All results are summarised in Figure 5 e). A preferential orientation appears with a maximum relative frequency (calculated

degree by degree) of 0.82% and a minimum of 0.38%. It illustrates the expected anisotropy of non-woven materials at the composite scale. This orientation anisotropy appears to be lower than the pure flax fibres non-woven preform analysed with the same technique by Gager et al. [21]. This can be explained by the presence of fine PLA fibres in our non-woven preform, modifying the flax fibre alignment during the calendaring process. The mean experimental curve, equation (4) developed by Neckar and Das [7], is used to fit experimental data (fig. 5.e).

$$f(\theta) = \frac{1}{\pi}\frac{C}{C^2 - (C^2 - 1)cos^2(\theta)} + q \quad (4)$$

where f(θ) is the fibre frequency at an angle θ taken between -90° and +90°, *C* is the fitting parameter corresponding to the anisotropy of the non-woven, and the offset is corrected via the parameter *q*. The fit was done by lowering the sum of the difference between experimental and model at each orientation, leading to *C* = 1.84 and *q* = 0.235%. As the trend curve is symmetric, it is preferred over the experimental curve for the micro-mechanical development in section 3.2.3.

3.2. Mechanical characterisation and prediction of non-woven composite

Fibre orientation is a key parameter affecting mechanical properties; its direct analysis is possible through expensive and time-consuming 3D investigations such as micro-CT. In contrast, using mechanical property measurements as an indirect method to ascertain fibre orientation may be faster, easier, and lower-cost. To check the relevancy of this alternative method, off-axis tensile experiments are compared to a theoretical prediction using laminate theory as described by Halpin and Pagano [12]. The orientation data for the non-woven composites analysed in the preceding sections

246 are matched with a theoretical model, which is used to implement a laminate with 181
247 distinct laminas (from -90 to +90) with a thickness weighted by the relative orientation
248 frequency. As symmetric lay-up is required, each ply is made of an angle and its
249 symmetric counterpart. The laminate creation is summarised in S.I. Figure 3.

250 *3.2.1. Angle influence on the tensile response of non-woven composite*

251 To study anisotropy in tensile properties arising from fibre orientation, experimental
252 measurements are presented in Table I and Figure 6. As expected, the loading angle
253 influences the material's response. A decrease in stiffness and strength of 40.5% and
254 47.3%, respectively, are observed between the orientations 0° and 90°, see Figure 7
255 and Table I. This confirms the anisotropy of this material. Furthermore, the mechanical
256 properties of the non-woven composite stay unchanged after a critical angle of 67.5°,
257 being equal to the transverse properties.

258 *3.2.2. Flax fibres properties for laminate theory*

259 Input values greatly impact micro-mechanical models, especially for plant fibre whose
260 values have a larger scatter. Indeed, regarding the longitudinal Young's modulus of
261 elementary flax fibres, it is possible to find literature values ranging from 36 GPa to 75
262 GPa [25,26]. Noting this scatter in data, two sets of values are considered here. The
263 first one is directly extracted from literature, presented in
264 Table II. The second one is obtained experimentally through back-calculation of UD
265 flax/PLA composite.
266 Table II presents the mechanical properties of these UD composites and the back-
267 calculated flax fibre properties for each UD composite. Comparing this data with the
268 literature, flax fibres longitudinal modulus is similar, whereas its transverse and shear

269 modulus obtained are lower. Thus, the thermal history of the fibres and the
270 compaction during the process may have impacted the structure of the flax fibres as
271 well as their mechanical properties.
272 Furthermore, both bundles and shives have been considered as 'fibres' during the
273 back-calculation. They generally have lower transverse and shear properties than
274 elementary flax fibres.
275 The reinforcement distribution inside the composite is also irregular, leading to some
276 regions of higher stress distribution than the theoretical approach. Additionally, as a
277 high volume fraction is achieved, some contact between fibres are present. These
278 contact points will be damaged during processing, damaging the fibres.

279 *3.2.3. Influence of non-woven structure on its mechanical properties*

280 Comparing the laminate theory models with the experimental data will inform us
281 whether off-axis tensile tests can be used to predict the fibre orientation of non-woven
282 flax composite. For each set of values, the mechanical properties of a ply are obtained
283 using the rule of mixture for the longitudinal direction and the Poisson's ratio and
284 using Halpin-Tsaï [27] for the transverse and shear moduli. Furthermore, as discussed
285 in section 3.1.1, porosity is present and has to be taken into account. We use the
286 hydrostatic balance-obtained single porosity value and assume that it is concentrated
287 in the matrix. This induces that the porosity inside shives is assimilated to be matrix
288 porosity. Equation (5), developed by Madsen et al. [16], is used to account for the
289 effect of matrix porosity on mechanical properties,

$$P_{m,real} = P_{m,bulk}.\left(1 - V_p\right)^2 \quad (5)$$

290 with *P* representing any mechanical property, V_p the volume fraction of porosity and
291 subscripts $_{m, bulk}$ and $_{m, real}$ denoting the bulk matrix and the matrix with porosity. Once
292 the ply properties are obtained, the laminate is built as explained previously, and the
293 mechanical properties of the equivalent composite are found. For each set of values,
294 the model generated a non-woven composite's tangent modulus versus orientation
295 curve. The range between both is represented in Figure 7 (grey area). The modulus in
296 the machine direction (0°) is well-predicted, falling between both models. A small
297 deviation appears for 22.5° and 45°, but the models stay close to the experimental
298 value.
299 However, increasing the orientation further to 45° leads to an overestimation. This
300 deviation at high orientations is principally due to the assumptions and simplifications
301 used for the model compared to reality. First of all, the model considers an in-plane
302 orientation. It is relevant for machine direction due to a stretching induced by the
303 manufacturing process. However, this stretching is less or not present in other
304 directions. That is why a slight out-of-plane orientation exists, needed for handling the
305 non-woven preform.
306 Additionally, the model does not consider the reinforcement effect of bundles. A
307 bundle present a higher diameter than elementary flax fibres and an irregular
308 geometry (fluctuating circularity, section and length), increasing the heterogeneity of
309 the composite structure. Bundles behaviour depends on its cohesion, meaning the
310 middle lamella properties. The latter impacts predominantly the composite properties
311 reliant on matrix and interface (such as transverse tensile properties). Furthermore, a
312 small number of shives were detected, adding heterogeneity in the structure too.

What is more, the manufacturing process smashes the shives. This transversal smashing creates damages in this porous structure, decreasing the transverse properties of shives. Furthermore, the model used here is based on an assumption of linear behaviour. However, it is known that elementary flax fibres do not have a linear longitudinal behaviour [28]. The transverse tensile behaviour of elementary flax fibres is still obscure as it is harsh to make some relevant tests at this micro-scale. In the non-woven composite, fibres are oriented but are also curved. This curvature is not considered in our orientation analysis, but it is known to have a non-negligible impact on the composite behaviour.

Finally, it appears that the anisotropy increases with fibre volume fraction, as observed in Figure 8. This new manufacturing process of non-woven preform allows overtaking in machine direction literature value without decreasing the stiffness significantly in cross-direction.

4. Conclusion

The complex microarchitecture of a non-woven flax/PLA composite with 50%wt of flax fibres was described thanks to micro-CT analysis. The microstructural observations show porosity and reveal the preferential orientation of the fibres inside the composite in the machine direction. This anisotropy was also measured through off-axis tensile tests. The mechanical properties highlight a clear anisotropy where transversal properties are 60% of the longitudinal properties. Both anisotropy characterisations are compared using micro-mechanics and laminate theory to predict the mechanical properties from the micro-CT orientation analysis.

It is found that off-axis tensile tests could be used to predict the fibre orientation distribution in a non-woven composite indirectly. This is interesting as tensile tests are much cheaper, faster and convenient to perform than micro-CT analysis. Industrially, it could be used for quality control of a production line or as a tool to develop new non-woven preforms with specific flax fibres orientation. The comparison of several set-up machinery or even manufacturing processes could also be handled.

However, some deviation is apparent between experimental data and micro-mechanical prediction because of the complexity of describing a flax composite due to the presence of flax bundles, shives, curved fibres, potential out-of-plane orientation of fibres, and also compounding effects from processing/thermal history. It may be of interest to further develop the models and ascertain their consistency with experimental data by examining the specific influence of shives and degree of flax fibre individualisation on the mechanical properties of non-woven flax composites. However, this may be experimentally challenging as flax preform and fibre quality, degree of fibre individualisation and quantity of shives are inherently interlinked.

Acknowledgements

Authors thank Interreg V.A Cross-Channel Programme for funding this work through our project, FLOWER (Grant number: 23; http://flower-project.eu). The authors also thank Dr D. Legland (INRAE) for developing the granulometry orientation analysis method.

References:

[1] S.V. Joshi, L.T. Drzal, A.K. Mohanty, S. Arora, Are natural fiber composites environmentally superior to glass fiber reinforced composites?, Composites Part

A: Applied Science and Manufacturing. 35 (2004) 371–376. https://doi.org/10.1016/j.compositesa.2003.09.016.

[2] A. Lefeuvre, A. Bourmaud, C. Morvan, C. Baley, Tensile properties of elementary fibres of flax and glass: Analysis of reproducibility and scattering, Materials Letters. 130 (2014) 289–291. https://doi.org/10.1016/j.matlet.2014.05.115.

[3] A.K. Bledzki, O. Faruk, V.E. Sperber, Cars from Bio-Fibres, Macromolecular Materials and Engineering. 291 (2006) 449–457. https://doi.org/10.1002/mame.200600113.

[4] N. Martin, P. Davies, C. Baley, Evaluation of the potential of three non-woven flax fiber reinforcements: Spunlaced, needlepunched and paper process mats, Industrial Crops and Products. 83 (2016) 194–205. https://doi.org/10.1016/j.indcrop.2015.10.008.

[5] V.M. Ghorpade, A. Gennadios, M.A. Hanna, Laboratory composting of extruded poly(lactic acid) sheets, Bioresource Technology. 76 (2001) 57–61. https://doi.org/10.1016/S0960-8524(00)00077-8.

[6] D. Pantaloni, D. Shah, C. Baley, A. Bourmaud, Monitoring of mechanical performances of flax non-woven biocomposites during a home compost degradation, Polymer Degradation and Stability. 177 (2020) 109166. https://doi.org/10.1016/j.polymdegradstab.2020.109166.

[7] B. Neckář, D. Das, Modelling of fibre orientation in fibrous materials, The Journal of The Textile Institute. 103 (2012) 330–340. https://doi.org/10.1080/00405000.2011.578357.

[8] M. Miao, M. Shan, Highly aligned flax/polypropylene non-woven preforms for thermoplastic composites, Composites Science and Technology. 71 (2011) 1713–1718. https://doi.org/10.1016/j.compscitech.2011.08.001.

[9] N. Graupner, F. Beckmann, F. Wilde, J. Müssig, Using synchroton radiation-based micro-computer tomography (SR μ-CT) for the measurement of fibre orientations in cellulose fibre-reinforced polylactide (PLA) composites, J Mater Sci. 49 (2014) 450–460. https://doi.org/10.1007/s10853-013-7724-8.

[10] R.A. Smith, L.J. Nelson, N. Xie, C. Fraij, S.R. Hallett, Progress in 3D characterisation and modelling of monolithic carbon-fibre composites, Insight. 57 (2015) 131–139. https://doi.org/10.1784/insi.2014.57.3.131.

[11] H. Krenchel, Fibre reinforcement; theoretical and practical investigations of the elasticity and strength of fibre-reinforced materials, (1964).

[12] J.C. Halpin, N.J. Pagano, The Laminate Approximation for Randomly Oriented Fibrous Composites, Journal of Composite Materials. 3 (1969) 720–724. https://doi.org/10.1177/002199836900300416.

[13] J. Merotte, A. Le Duigou, A. Bourmaud, K. Behlouli, C. Baley, Mechanical and acoustic behaviour of porosity controlled randomly dispersed flax/PP biocomposite, Polymer Testing. 51 (2016) 174–180. https://doi.org/10.1016/j.polymertesting.2016.03.002.

[14] M. Mehdikhani, L. Gorbatikh, I. Verpoest, S.V. Lomov, Voids in fiber-reinforced polymer composites: A review on their formation, characteristics, and effects on mechanical performance, Journal of Composite Materials. 53 (2019) 1579–1669. https://doi.org/10.1177/0021998318772152.

[15] B. Madsen, A. Thygesen, H. Lilholt, Plant fibre composites – porosity and volumetric interaction, Composites Science and Technology. 67 (2007) 1584–1600. https://doi.org/10.1016/j.compscitech.2006.07.009.

[16] B. Madsen, A. Thygesen, H. Lilholt, Plant fibre composites – porosity and stiffness, Composites Science and Technology. 69 (2009) 1057–1069. https://doi.org/10.1016/j.compscitech.2009.01.016.

[17] D.U. Shah, P.J. Schubel, M.J. Clifford, P. Licence, The tensile behavior of off-axis loaded plant fiber composites: An insight on the nonlinear stress-strain response, Polymer Composites. 33 (2012) 1494–1504. https://doi.org/10.1002/pc.22279.

[18] D. Pantaloni, A.L. Rudolph, D.U. Shah, C. Baley, A. Bourmaud, Interfacial and mechanical characterisation of biodegradable polymer-flax fibre composites, Composites Science and Technology. 201 (2021) 108529. https://doi.org/10.1016/j.compscitech.2020.108529.

[19] C. Kergariou, A.L. Duigou, V. Popineau, V. Gager, A. Kervoelen, A. Perriman, H. Saidani-Scott, G. Allegri, T.H. Panzera, F. Scarpa, Measure of porosity in flax fibres reinforced polylactic acid biocomposites, Composites Part A: Applied Science and Manufacturing. (2020) 106183. https://doi.org/10.1016/j.compositesa.2020.106183.

[20] M. Le Gall, P. Davies, N. Martin, C. Baley, Recommended flax fibre density values for composite property predictions, Industrial Crops and Products. 114 (2018) 52–58. https://doi.org/10.1016/j.indcrop.2018.01.065.

[21] V. Gager, D. Legland, A. Bourmaud, A. Le Duigou, F. Pierre, K. Behlouli, C. Baley, Oriented granulometry to quantify fibre orientation distributions in synthetic and plant fibre composite preforms, Industrial Crops and Products. 152 (2020) 112548. https://doi.org/10.1016/j.indcrop.2020.112548.

[22] C. Goudenhooft, A. Bourmaud, C. Baley, Flax (Linum usitatissimum L.) Fibers for Composite Reinforcement: Exploring the Link Between Plant Growth, Cell Walls Development, and Fiber Properties, Front. Plant Sci. 10 (2019). https://doi.org/10.3389/fpls.2019.00411.

[23] P. Evon, B. Barthod-Malat, M. Grégoire, G. Vaca-Medina, L. Labonne, S. Ballas, T. Véronèse, P. Ouagne, Production of fiberboards from shives collected after continuous fiber mechanical extraction from oleaginous flax, Journal of Natural Fibers. 16 (2019) 453–469. https://doi.org/10.1080/15440478.2017.1423264.

[24] L. Nuez, J. Beaugrand, D.U. Shah, C. Mayer-Laigle, A. Bourmaud, P. D'Arras, C. Baley, The potential of flax shives as reinforcements for injection moulded - polypropylene composites, Industrial Crops and Products. 148 (2020) 112324. https://doi.org/10.1016/j.indcrop.2020.112324.

[25] C. Baley, A. Le Duigou, C. Morvan, A. Bourmaud, Tensile properties of flax fibers, in: Handbook of Properties of Textile and Technical Fibres, Elsevier, 2018: pp. 275–300. https://doi.org/10.1016/B978-0-08-101272-7.00008-0.

443 [26] C. Baley, A. Bourmaud, Average tensile properties of French elementary flax
444 fibers, Materials Letters. 122 (2014) 159–161.
445 https://doi.org/10.1016/j.matlet.2014.02.030.
446 [27] J.C.H. Affdl, J.L. Kardos, The Halpin-Tsai equations: A review, Polymer Engineering
447 & Science. 16 (1976) 344–352. https://doi.org/10.1002/pen.760160512.
448 [28] A. Lefeuvre, A. Bourmaud, C. Morvan, C. Baley, Elementary flax fibre tensile
449 properties: Correlation between stress–strain behaviour and fibre composition,
450 Industrial Crops and Products. 52 (2014) 762–769.
451 https://doi.org/10.1016/j.indcrop.2013.11.043.
452 [29] E. Bodros, I. Pillin, N. Montrelay, C. Baley, Could biopolymers reinforced by
453 randomly scattered flax fibre be used in structural applications?, Composites
454 Science and Technology. 67 (2007) 462–470.
455 https://doi.org/10.1016/j.compscitech.2006.08.024.
456 [30] S. Alimuzzaman, R.H. Gong, M. Akonda, Nonwoven polylactic acid and flax
457 biocomposites, Polymer Composites. 34 (2013) 1611–1619.
458 https://doi.org/10.1002/pc.22561.
459 [31] M. Akonda, S. Alimuzzaman, D.U. Shah, A.N.M.M. Rahman, Physico-Mechanical,
460 Thermal and Biodegradation Performance of Random Flax/Polylactic Acid and
461 Unidirectional Flax/Polylactic Acid Biocomposites, Fibers. 6 (2018) 98.
462 https://doi.org/10.3390/fib6040098.
463 [32] B. Bax, J. Müssig, Impact and tensile properties of PLA/Cordenka and PLA/flax
464 composites, Composites Science and Technology. 68 (2008) 1601–1607.
465 https://doi.org/10.1016/j.compscitech.2008.01.004.
466 [33] F. Roussière, C. Baley, G. Godard, D. Burr, Compressive and Tensile Behaviours of
467 PLLA Matrix Composites Reinforced with Randomly Dispersed Flax Fibres, Appl
468 Compos Mater. 19 (2012) 171–188. https://doi.org/10.1007/s10443-011-9189-8.
469 [34] K. Oksman, Mechanical Properties of Natural Fibre Mat Reinforced Thermoplastic,
470 Applied Composite Materials. 7 (2000) 403–414.
471 https://doi.org/10.1023/A:1026546426764.

[35] J. Andersons, E. Spārniņš, R. Joffe, Stiffness and strength of flax fiber/polymer matrix composites, Polymer Composites. 27 (2006) 221–229. https://doi.org/10.1002/pc.20184.

[36] K.-P. Mieck, R. Lützkendorf, T. Reussmann, Needle-Punched hybrid non-wovens of flax and ppfibers—textile semiproducts for manufacturing of fiber composites, Polymer Composites. 17 (1996) 873–878. https://doi.org/10.1002/pc.10680.

[37] C. Baley, Y. Perrot, F. Busnel, H. Guezenoc, P. Davies, Transverse tensile behaviour of unidirectional plies reinforced with flax fibres, Materials Letters. 60 (2006) 2984–2987. https://doi.org/10.1016/j.matlet.2006.02.028.

[38] C. Baley, A. Kervoëlen, A. Le Duigou, C. Goudenhooft, A. Bourmaud, Is the low shear modulus of flax fibres an advantage for polymer reinforcement?, Materials Letters. 185 (2016) 534–536. https://doi.org/10.1016/j.matlet.2016.09.067.

[39] C. Baley, Fibres naturelles de renfort pour matériaux composites. sl: Techniques de l'ingénieur, Ref. AM. 5 (2014) 130.

Figures:

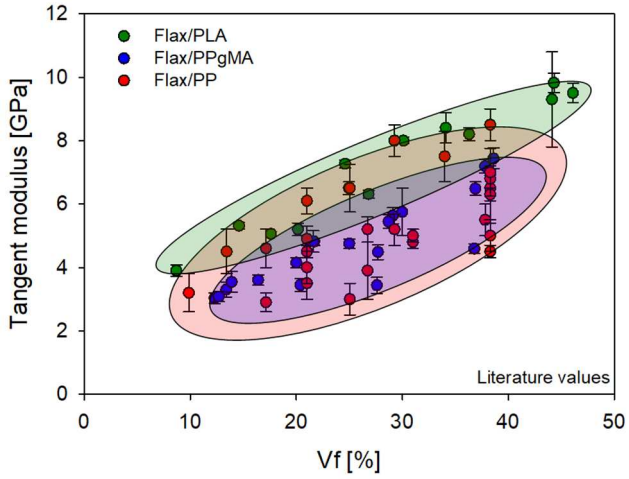

Figure 1: Graphical presentation of literature review of the mechanical properties of non-woven flax composites reinforcing PLA [29–33] ; PP [13,16,34–36] ; MAPP [4,29]

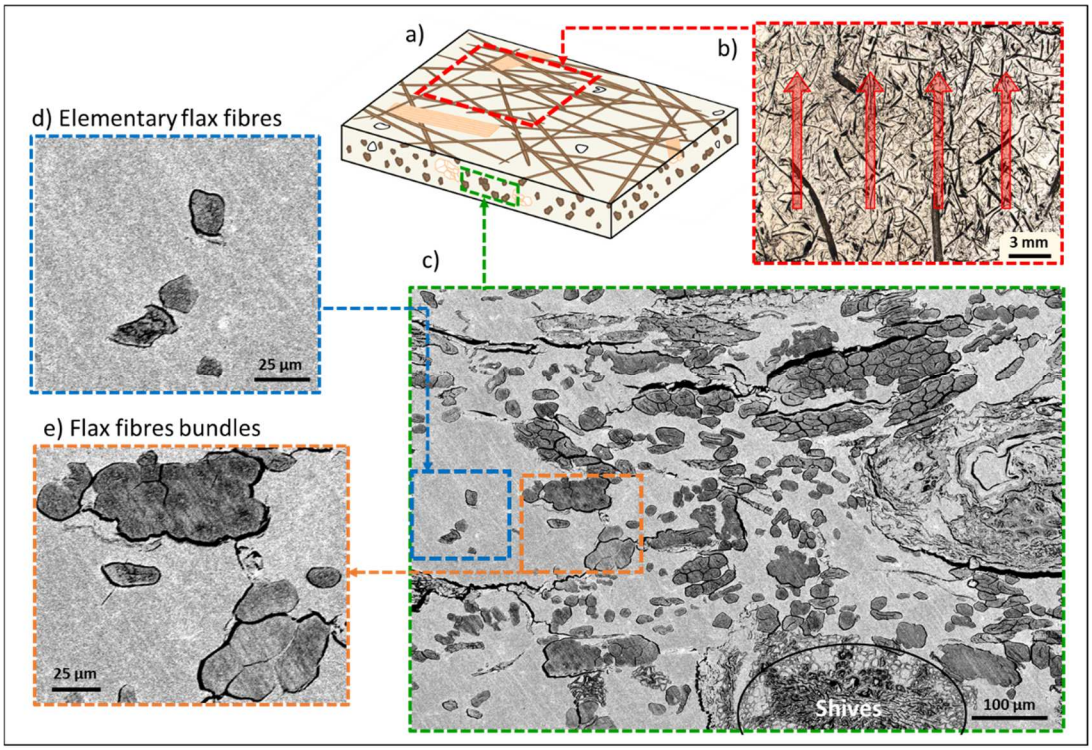

Figure 2: SEM observation of the flax/PLA non-woven investigated, a) a schematic representation of the analysed sample, b) upper observation, showing preferential fibre orientation (red arrows), c) transverse observation, cracks might be due to water polishing, d) zoom on elementary flax fibres, e) zoom on flax bundles.

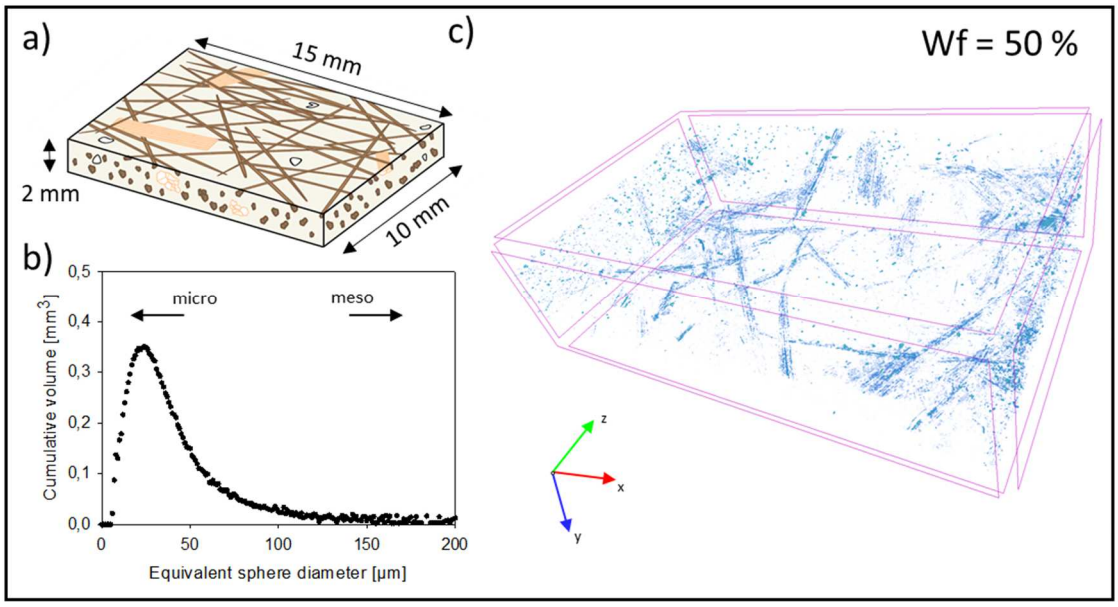

496

497 Figure 3: Porosity analysis by micro-CT a) schema of the analysed sample, b) analysis of

498 porosity size, c) the micro-CT 3D view of porosity.

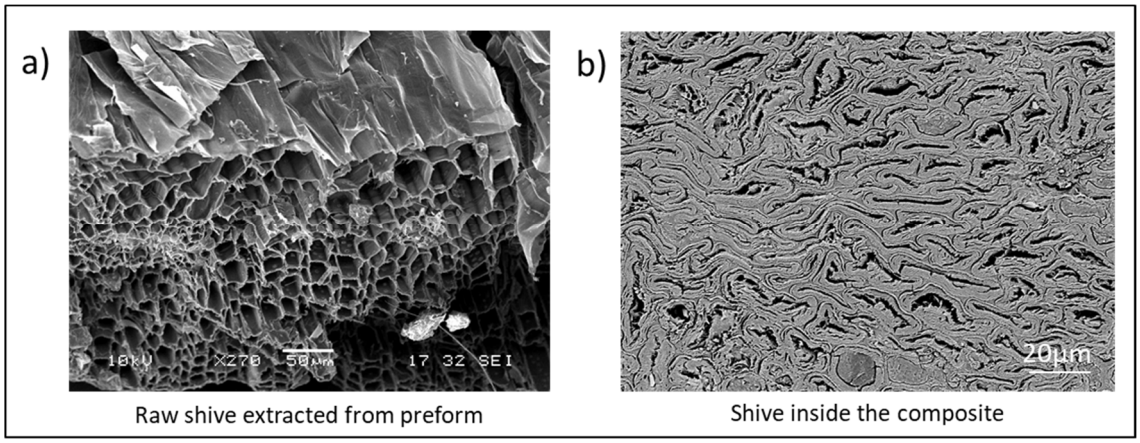

499

500 Figure 4: SEM observation of a shive a) before the composite manufacturing step with

501 open cells, b) after composite manufacturing, showing collapsed cells.

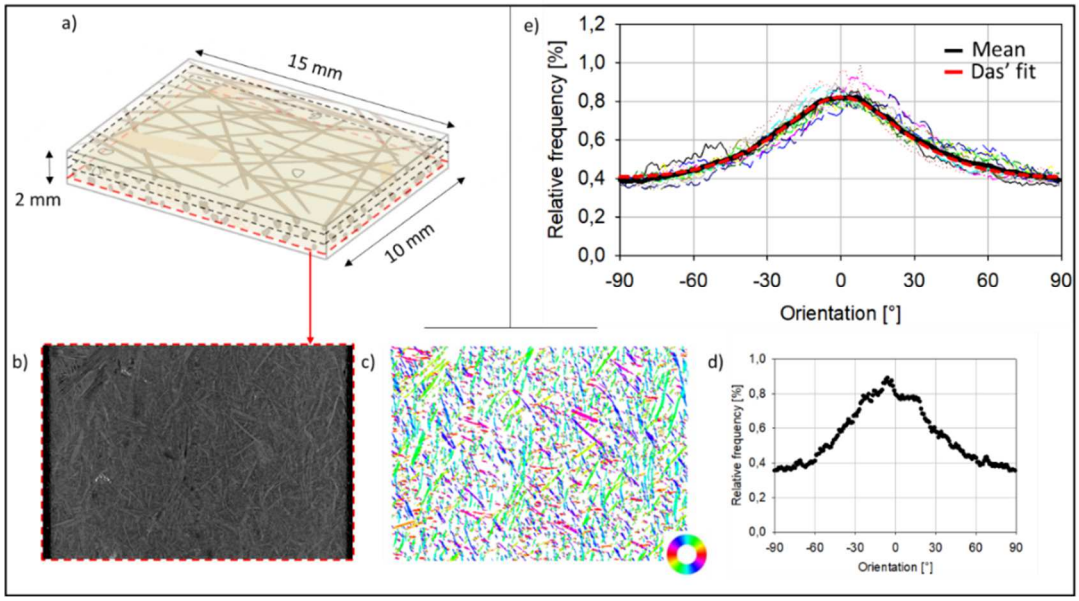

Figure 5: Orientation analysis. a) sample schema with slices (marked by dotted line) investigated, b) micro-CT image analysed for local fibre orientation, c) orientation analysis representation of micro-CT image (each colour represents an orientation), d) Orientation frequency histogram of one micro-CT slice, e) global orientation analysis of the composite, based on the mean orientation (black) of twelve micro-CT slices (dotted coloured lines). An interpolation [7], based on the mean value, is shown in red dotted lines.

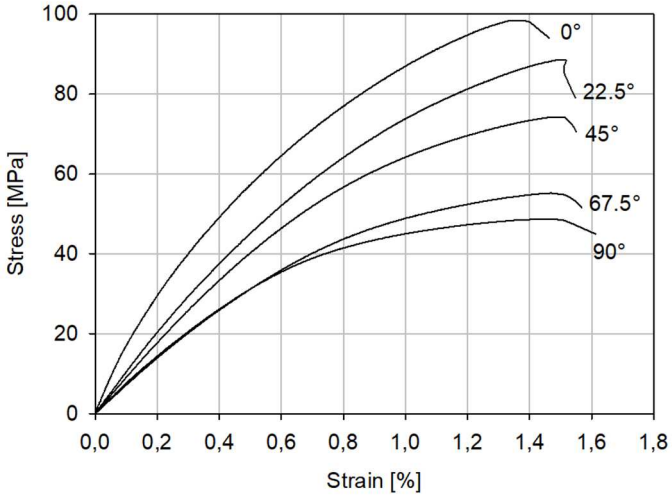

510

511 Figure 6: Tensile behaviour of non-woven flax/PLA with 50 wt% of fibres at several

512 loading angles. The 0° refer to the machine direction and the 90° to the cross direction.

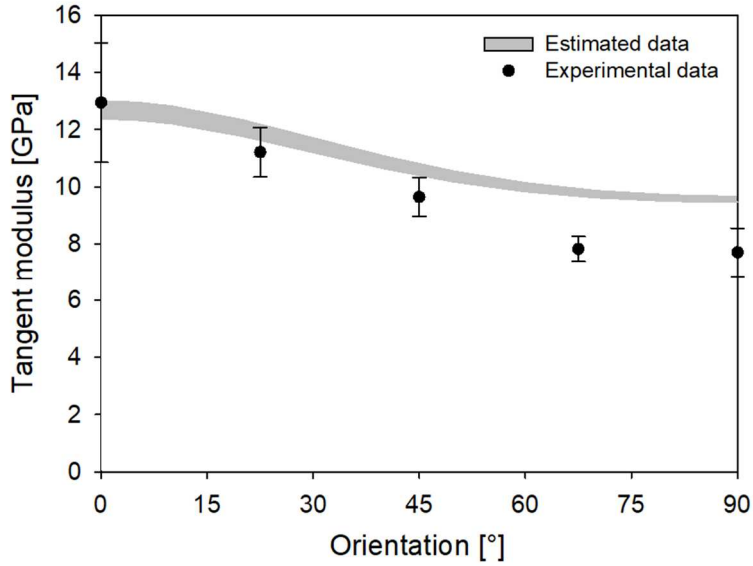

513

514 Figure 7: Evolution of the tangent modulus with loading orientation for non-woven

515 flax/PLA with 50wt% of fibres tested in tension.

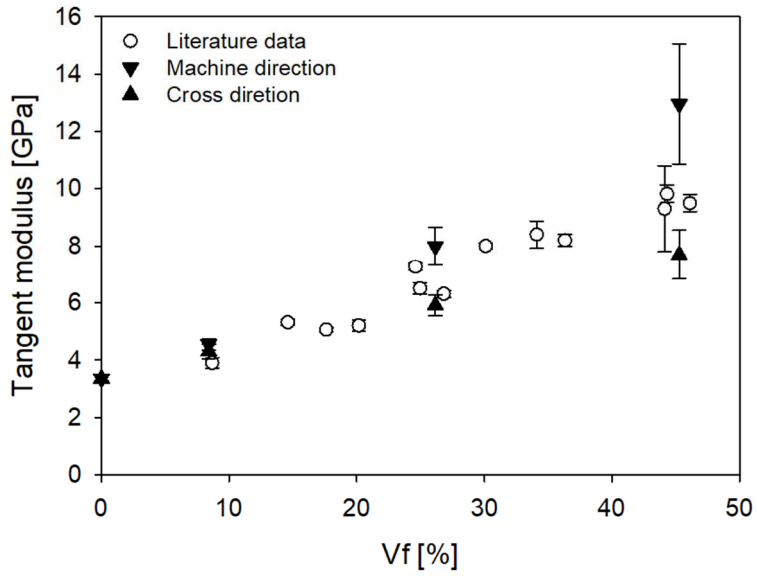

516

517 Figure 8: Evolution of tangent modulus with fibre volume fraction, with measurements

518 in the orthogonal machine and cross directions presenting anisotropy. A comparison

519 with literature data is also presented.

520 **Tables:**

521 Table I: Experimental values of longitudinal, transversal and off-axis tensile tests on

522 non-woven flax/PLA with 50 wt% of fibres.

Angle [°]	Tangent modulus [GPa]	Strength [MPa]	Strain at rupture [%]
0	12.95 ± 2.09	90.0 ± 6.1	1.44 ± 0.27
22.5	11.21 ± 0.87	84.9 ± 4.3	1.48 ± 0.27
45	9.64 ± 0.67	69.6 ± 6.5	1.30 ± 0.31
67.5	7.82 ± 0.44	53.2 ± 4.1	1.38 ± 0.25
90	7.70 ± 0.85	47.4 ± 4.4	1.25 ± 0.26

523

524 Table II: Flax/PLA UD composite mechanical properties used to obtain mechanical

525 properties of flax via a back-calculation method : rule of mixture for longitudinal

526 modulus (E_l) and Poisson's ratio (ν_{lt}), Halpin Tsaï for shear modulus (G_{lt}) and transverse

527 modulus (E_t).

	V_f [%]	E_l [GPa]	E_t [GPa]	G_{lt} [GPa]	ν_{lt} [-]
Experimental values for Unidirectional Composites	0	3.73	3.73	1.31	0.41
	30	20.09	4.17	1.76	-
	40	25.98	4.29	1.88	0.39
	50	27.47	4.13	2.04	0.37
Flax fibres properties by back-calculation	30	58.26	5.35	3.76	-
	40	59.34	5.24	3.42	0.35
	50	51.21	4.56	3.33	0.33
Mean back calculated flax fibres value		56.2 ± 3.6	5.05 ± 0.35	3.50 ± 0.18	0.34 ± 0.01
Literature value for flax fibres		52.5 ± 8.6 [26]	8 ± 3 [37]	2.5 ± 0.2 [38]	0.48 [39]

528

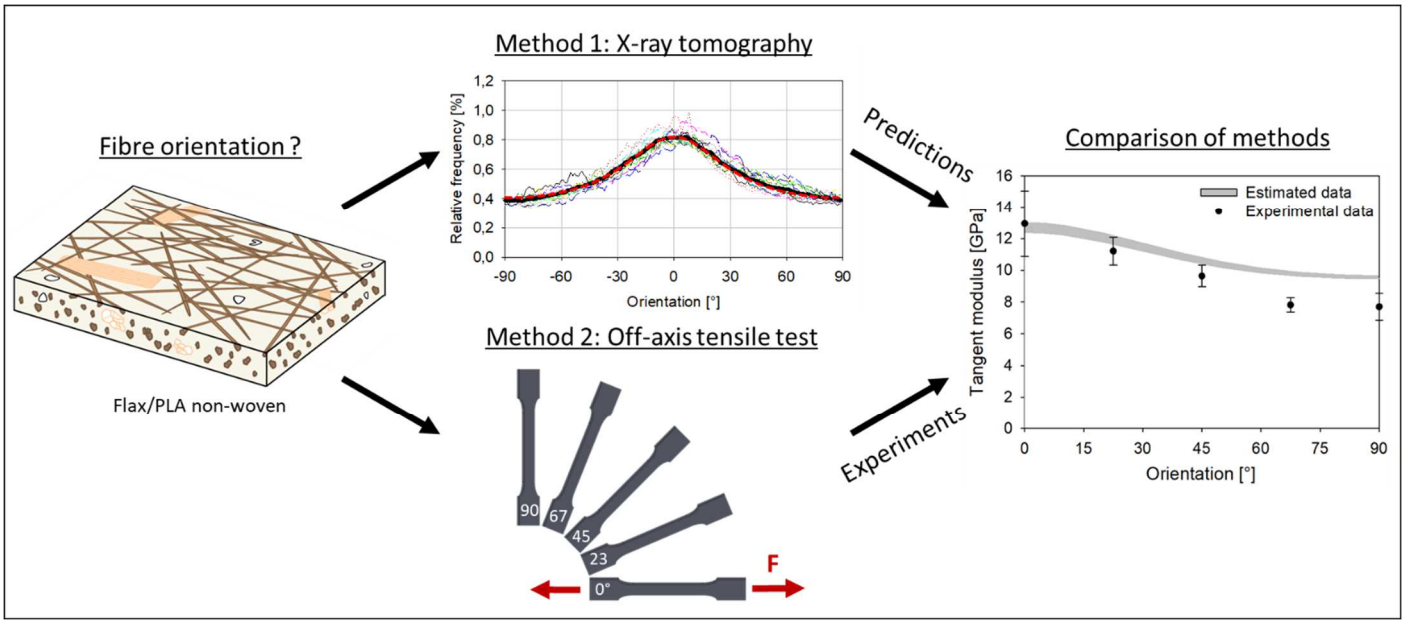
Fibre orientation ?
Flax/PLA non-woven
Method 1: X-ray tomography
Relative frequency [%]
Orientation [°]
Method 2: Off-axis tensile test
90
67
45
23
0°
F
Predictions
Experiments
Comparison of methods
Estimated data
Experimental data
Tangent modulus [GPa]
Orientation [°]